

## Discovery of cryptic largimycins in *Streptomyces* reveals novel biosynthetic avenues enriching the structural diversity of the leinamycin family

Adriana Becerril, Ignacio Pérez-Victoria, Suhui Ye, Alfredo F Braña,  
Jesus Martin, Fernando Reyes, Jose A. Salas, and Carmen Méndez

*ACS Chem. Biol.*, **Just Accepted Manuscript** • DOI: 10.1021/acscchembio.0c00160 • Publication Date (Web): 20 Apr 2020

Downloaded from [pubs.acs.org](https://pubs.acs.org) on April 20, 2020

### Just Accepted

“Just Accepted” manuscripts have been peer-reviewed and accepted for publication. They are posted online prior to technical editing, formatting for publication and author proofing. The American Chemical Society provides “Just Accepted” as a service to the research community to expedite the dissemination of scientific material as soon as possible after acceptance. “Just Accepted” manuscripts appear in full in PDF format accompanied by an HTML abstract. “Just Accepted” manuscripts have been fully peer reviewed, but should not be considered the official version of record. They are citable by the Digital Object Identifier (DOI®). “Just Accepted” is an optional service offered to authors. Therefore, the “Just Accepted” Web site may not include all articles that will be published in the journal. After a manuscript is technically edited and formatted, it will be removed from the “Just Accepted” Web site and published as an ASAP article. Note that technical editing may introduce minor changes to the manuscript text and/or graphics which could affect content, and all legal disclaimers and ethical guidelines that apply to the journal pertain. ACS cannot be held responsible for errors or consequences arising from the use of information contained in these “Just Accepted” manuscripts.

1  
2  
3 1  
4  
5 2  
6  
7 3 **Discovery of cryptic largimycins in *Streptomyces* reveals novel biosynthetic avenues**  
8 **enriching the structural diversity of the leinamycin family**  
9  
10 5  
11 6  
12 7  
13 8  
14 9

15 8  
16 9  
17 9  
18  
19 10 **Adriana Becerril,<sup>†,‡,§</sup> Ignacio Pérez-Victoria,<sup>#,§</sup> Suhui Ye, <sup>†,‡</sup> Alfredo F. Braña, <sup>†,‡</sup> Jesús**  
20  
21 11 **Martín, <sup>#</sup> Fernando Reyes, <sup>#</sup> José A. Salas<sup>†,‡</sup> and Carmen Méndez<sup>\*,†,‡</sup>**  
22  
23 12  
24 13  
25 13  
26 14  
27 14  
28 15  
29 15  
30 16  
31 16  
32 17  
33 17

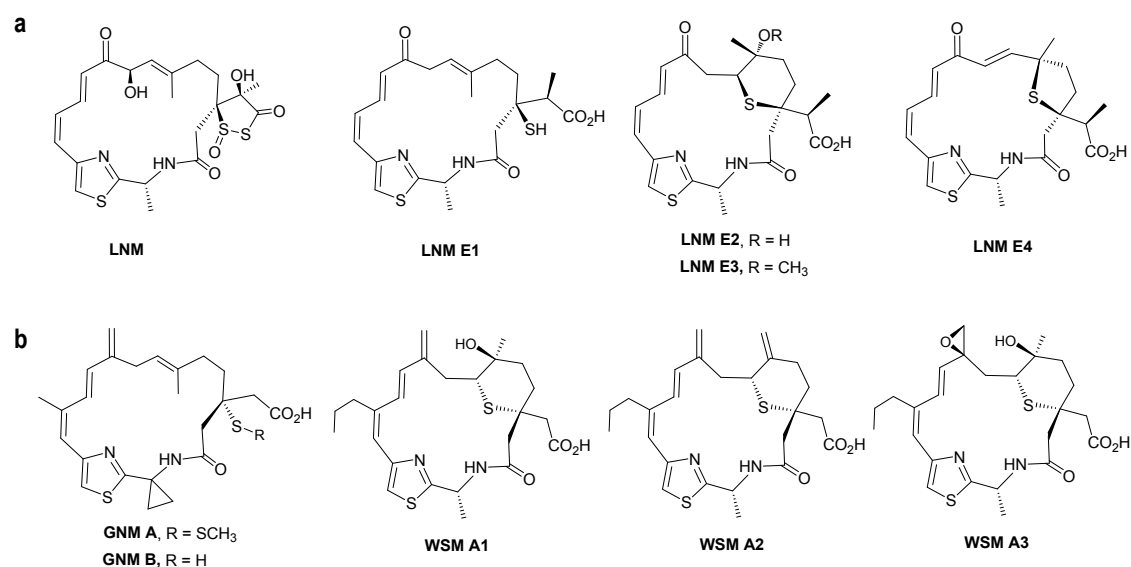
34 18 <sup>†</sup>Departamento de Biología Funcional e Instituto Universitario de Oncología del Principado de  
35 Asturias (I.U.O.P.A), Universidad de Oviedo, Oviedo, Spain  
36  
37 19 <sup>‡</sup>Instituto de Investigación Sanitaria de Asturias (ISPA), Oviedo, Spain  
38  
39 20 <sup>#</sup>Fundación MEDINA, Centro de Excelencia en Investigación de Medicamentos Innovadores en  
40  
41 21 Andalucía, Armilla, Granada, Spain.  
42  
43 22 <sup>§</sup>These authors contributed equally  
44  
45 23  
46  
47 24  
48  
49 25 **\* Correspondence:** Carmen Méndez ([cmendezf@uniovi.es](mailto:cmendezf@uniovi.es))  
50  
51  
52  
53  
54  
55  
56  
57  
58  
59  
60

1  
2  
3 27 **ABSTRACT**  
4

5 28 Largimycins are hybrid nonribosomal peptide-polyketides that constitute a new group of  
6 29 metabolites in the leinamycin family of natural products displaying unique structural features such  
7  
8 30 as containing an oxazole instead of a thiazole ring or being oxime ester macrocycles,  
9  
10 31 unprecedented in Nature, rather than macrolactams. Their discovery in *Streptomyces argillaceus*  
11  
12 32 and *Streptomyces canus* has relied on the activation of two homologous silent gene clusters by  
13  
14 33 overexpressing a transcriptional activator and cultivating in specific media. The proposed  
15  
16 34 biosynthesis of largimycins includes the key action of the oxidoreductase LrgO, responsible for  
17  
18 35 the formation of the oxime group involved in macrocyclization, and two putative cryptic  
19  
20 36 biosynthetic steps consisting in chlorination of L-Thr by the NRPS loading module and  
21  
22 37 incorporation of an olefinic exomethylene group by LrgJ PKS. The discovery of largimycins  
23  
24 38 uncovers novel biosynthetic avenues employed by Nature to enrich the structural diversity of  
25  
26 39 leinamycins and provides tools for combinatorial biosynthesis.  
27  
28  
29  
30  
31  
32  
33  
34  
35  
36  
37  
38  
39  
40  
41  
42  
43  
44  
45  
46  
47  
48  
49  
50  
51  
52  
53  
54  
55  
56  
57  
58  
59  
60

1  
2  
3  
4  
5  
6  
7  
8  
9  
10  
11  
12  
13  
14  
15  
16  
17  
18  
19  
20  
21  
22  
23  
24  
25  
26  
27  
28  
29  
30  
31  
32  
33  
34  
35  
36  
37  
38  
39  
40  
41  
42  
43  
44  
45  
46  
47  
48  
49  
50  
51  
52

*Streptomyces* bacteria are a prolific source of natural products displaying some kind of bioactivity.<sup>1</sup> Many of these specialized metabolites are polyketides (PKs) and nonribosomal peptides (NRPs), including hybrid PK-NRPs. Leinamycin (LNM) is a remarkable example of such bioactive hybrid natural products.<sup>2</sup> It is characterized by a 1,3-dioxo-1,2-dithiolane moiety spirofused to thiazole-containing macrolactam ring (Figure 1a), and displays antitumor activity exerted through a novel mode of action rendering DNA damage.<sup>2,3</sup> The LNM macrolactam ring is synthesized by a hybrid nonribosomal peptide synthetase (NRPS)/acyltransferase (AT)-less type I polyketide synthase (PKS) featuring a novel pathway for PK  $\beta$ -alkylation and a didomain of unknown function (DUF)-cystein lyase domain (SH), which incorporates sulfur in the PK chain.<sup>4-6</sup> Since its discovery thirty years ago,<sup>2</sup> LNM has constituted the only known member of this class of compounds until the very recent discovery of two other members, the guanganmycins (GNMs) and the weishanmycins (WSMs) (Figure 1b).<sup>7</sup>



54 **Figure 1.** Structure of known leinamycin metabolites. a) leinamycins (LNMs). b) guanganmycins (GNMs) and weishanmycins (WSMs).

57  
58  
59  
60  
61  
62  
63  
64

Genome mining of *Streptomyces* species has untapped their enormous potential to produce specialized metabolites, based on the plethora of biosynthetic gene clusters (BGCs) identified.<sup>8</sup> However, most of these clusters are not (or only poorly) expressed under standard laboratory cultivation conditions. Several strategies have been developed to induce the expression of such silent BGCs, including the genetic manipulation and/or the modification of growth conditions, in order to identify their encoded metabolites.<sup>9-11</sup> Recently, genome mining of *Streptomyces argillaceus* ATCC 12956 has identified 31 putative BGCs.<sup>12</sup> In addition to the BGC for the antitumor mithramycin that had been previously cloned and characterized,<sup>13</sup> five cryptic BGCs



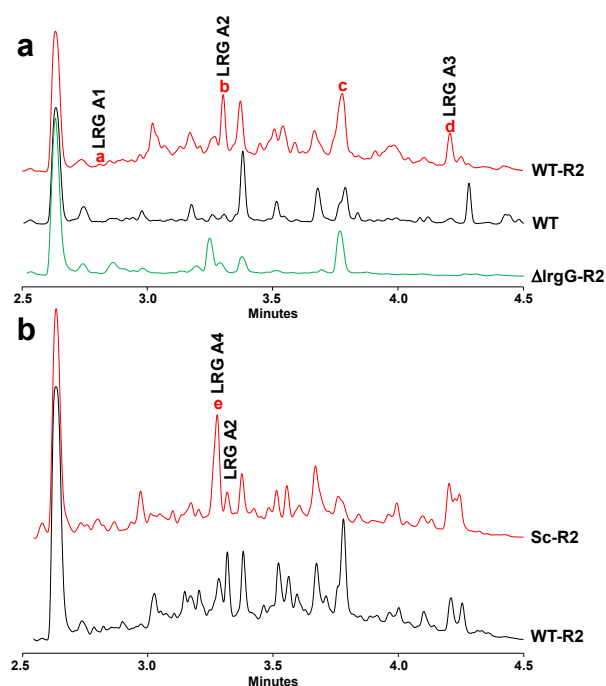
89 in R5A medium did not show any differential peak, indicating that cluster 11 was silent (data not  
90 shown); (ii) Activation of cluster 11 by overexpressing/deleting putative transcriptional regulators.

91  
92 **Table 1. Predicted functions of genes in the *Streptomyces argillaceus* *lrg* gene cluster**

| Gene product | aa   | Proposed function                        | Most similar protein (acc. number) | Identical aa (%) | Similar protein Lnm/Syr | Identical aa (%) |
|--------------|------|--|------------------------------------|------------------|-------------------------|------------------|
| ORF18        | 202  | Hypothetical protein                     | KUN87089.1                         | 94               |                         |                  |
| LrgT1        | 509  | MFS transporter                          | WP_100570177.1                     | 94               | LnmY                    | 40               |
| LrgR3        | 205  | TetR family transcriptional regulator    | WP_100570178.1                     | 93               |                         |                  |
| LrgP1        | 191  | Hypothetical protein                     | WP_100570179.1                     | 94               |                         |                  |
| LrgC1        | 452  | Cytochrome P450                          | WP_100570180.1                     | 93               |                         |                  |
| LrgR1        | 222  | Crp/Fnr family transcriptional regulator | WP_100570182.1                     | 96               | LnmO                    | 43               |
| LrgQ         | 250  | Phosphopantetheinyl transferase          | WP_100570183.1                     | 91               |                         |                  |
| LrgC2        | 433  | Cytochrome P450                          | WP_100570184.1                     | 97               | LnmA/LnmZ               | 36/36            |
| LrgR2        | 252  | Crp/Fnr family transcriptional regulator | WP_100570185.1                     | 90               | LnmO                    | 42               |
| LrgT2        | 437  | Sodium:proton exchanger                  | WP_100570186.1                     | 95               |                         |                  |
| LrgE         | 299  | Hypothetical protein                     | WP_100570187.1                     | 94               | LnmE/LnmH               | 48/34            |
| LrgM2        | 410  | Hydroxymethylglutaryl-CoA synthase       | WP_100570188.1                     | 97               | LnmM                    | 45               |
| LrgF         | 263  | Enoyl-CoA hydratase                      | WP_100570189.1                     | 97               | LnmF                    | 53               |
| LrgG         | 798  | AT-less acyltransferase/oxidoreductase   | WP_100570343.1                     | 91               | LnmG                    | 64               |
| LrgP2        | 316  | Hypothetical protein                     | WP_100570190.1                     | 97               | LnmH/LnmE               | 43/43            |
| LrgS         | 599  | NRPS (A-PCP)                             | WP_100570191.1                     | 95               | SyrB1                   | 46               |
| LrgH         | 314  | Halogenase                               | WP_100570344.1                     | 97               | SyrB2                   | 67               |
| LrgY         | 391  | Aminoacyltransferase                     | WP_100570192.1                     | 94               | SyrC                    | 43               |
| LrgI         | 4288 | hybrid NRPS/AT-less Type I PKS           | WP_100570193.1                     | 91               | LnmI                    | 51               |
| LrgJ         | 7340 | AT-less type I PKS                       | WP_100570194.1                     | 90               | LnmJ                    | 48               |
| LrgK         | 330  | acyltransferase/decarboxylase            | WP_100570195.1                     | 93               | LnmK                    | 54               |
| LrgL         | 87   | Acyl carrier protein                     | WP_100570196.1                     | 94               | LnmL                    | 66               |
| LrgM1        | 412  | Hydroxymethylglutaryl-CoA synthase       | WP_100570197.1                     | 93               | LnmM                    | 63               |
| LrgA         | 80   | Acyl carrier protein                     | WP_100570198.1                     | 97               |                         |                  |
| LrgD         | 423  | Beta-ketoacyl-ACP synthase               | WP_100570199.1                     | 95               |                         |                  |
| LrgN         | 253  | Type II thioesterase                     | WP_059300315.1                     | 90               | LnmN                    | 54               |
| LrgX         | 239  | N-acetylglucosaminyl deacetylase         | WP_100570201.1                     | 93               | LnmX                    | 56               |
| LrgZ         | 132  | Hypothetical protein                     | WP_079252697.1                     | 95               | LnmZ'                   | 34               |
| LrgW1        | 487  | 4-coumarate-CoA ligase                   | WP_100570203.1                     | 93               | LnmW                    | 44               |
| LrgR4        | 201  | TetR family transcriptional regulator    | WP_100570204.1                     | 88               |                         |                  |
| LrgO         | 395  | FAD-dependent oxidoreductase             | WP_100570205.1                     | 94               |                         |                  |
| LrgB         | 121  | Glyoxalase/bleomycin resistance protein  | WP_100570206.1                     | 93               |                         |                  |
| LrgW2        | 494  | 4-coumarate-CoA ligase                   | WP_100570207.1                     | 96               | LnmW                    | 42               |
| LrgC3        | 414  | Cytochrome P450                          | PJM93929.1                         | 96               | LnmA                    | 36               |
| ORF52        | 93   | Hypothetical protein                     | WP_033213698.1                     | 75               |                         |                  |
| ORF53        | 179  | Hypothetical protein                     | WP_100570209.1                     | 82               |                         |                  |
| ORF54        | 489  | Amino acid permease                      | WP_020126812.1                     | 93               |                         |                  |

93 A, adenilation domain; AT, acyltransferase domain; ACP, acyl carrier protein; MFS, major facilitator superfamily;  
94 NRPS, non-ribosomal peptide synthetase; PCP, peptidyl carrier protein; PKS, polyketide synthase. Lnm and Syr,  
95 leinamycin and syringomycin proteins.

Cluster 11 contains 6 genes for putative regulatory proteins, four of which located within the DNA region showing homology to the *Inm* BGC (Table 1). The putative activators *IrgR1* and *IrgR2* were independently expressed into *S. argillaceus* wild type strain generating *S. argillaceus* WT-R1 and *S. argillaceus* WT-R2 strains respectively, and mutants in the putative repressors *IrgR3* (*S. argillaceus*  $\Delta$ IrgR3) and in *IrgR4* (*S. argillaceus*  $\Delta$ IrgR4) were generated (see Supporting Information). Analyses of the metabolite profiles of these strains did not show any differential peak (data not shown) indicating that overexpression and/or deletion of single regulatory genes was not sufficient to activate cluster 11; (iii) Media screening. Composition of culture media greatly influences production of secondary metabolites.<sup>16</sup> Twenty-nine culture media, including the LNM production media LF1 and LF2,<sup>2</sup> were screened for activating cluster 11 (see Supporting Information). In two of them (SM19 and SM30) several differential peaks were detected in *S. argillaceus* WT-R2, being their intensity higher with SM30 medium (Figure 3a). This result indicated that the newly biosynthesized compounds are produced by *S. argillaceus* only when *IrgR2* is overexpressed and the recombinant strain is cultivated in specific culture media. The involvement of cluster 11 in their production was confirmed by overexpressing *IrgR2* into  $\Delta$ IrgG mutant, which showed that the key peaks detected in *S. argillaceus* WT-R2 were not detected in *S. argillaceus*  $\Delta$ IrgG-R2 (Figure 3a), confirming that these compounds are encoded by cluster 11. Improvement of production (about 75%) of the major compound (peak **b** in Figure 3a) could be achieved substituting glucose by molasses from rice, and this modified medium (SM30a) was chosen for all experiments thereafter.



116

1  
2  
3 **Figure 3.** Production of largimycins by *S. argillaceus* and *S. canus*. UPLC chromatograms (330  
4 nm) of ethyl acetate extracts of (a) *S. argillaceus* WT, *S. argillaceus* WT-R2, and *S. argillaceus*  
5  $\Delta$ lrgG-R2 strains cultivated in SM30; (b) *S. argillaceus* WT-R2 and *S. canus* WT-R2 (Sc-R2)  
6 strains cultivated in SM30a. Peaks with letters correspond to those largimycins (LRGs) selected  
7 for chemical characterization. Peaks for LRG A1, LRG A2, LRG A3 and LRG A4 are indicated.  
8  
9

10  
11  
12  
13 The induced compounds in *S. argillaceus* WT-R2 were named largimycins (LRGs). The three  
14 main compounds detected in ethyl acetate extracts (peaks **b-d** in Figure 3a) were purified  
15 together with the compound from peak **a**, which turned out to be produced in higher amounts  
16 after solid-phase extraction of the scaled-up broth. Compounds from peaks **a** and **b** were named  
17 LRG A1 (**1**) and LRG A2 (**2**) respectively (Figure 4a). Their structures were elucidated (see  
18 Supporting Information) after high-resolution mass spectrometry (HRMS) and 1D (<sup>1</sup>H) and 2D  
19 NMR spectroscopy, further assisted by comparison with the reported NMR data of known LNMs.  
20 Detailed analysis of the key correlations observed in the COSY and HMBC spectra (Figure 4b)  
21 combined with the determined molecular formulae rendered the full connectivity of **1** and **2**  
22 confirming the structural relation with known LNMs. The *Z* stereochemistry of the oxime double  
23 bond was established on the basis of the observed  $\delta_C$  for C-18 which would be 2-4 ppm smaller  
24 in case of the *E* geometric isomers,<sup>17</sup> as indicated by comparison with model compounds and  
25 empirically-based prediction of <sup>13</sup>C NMR chemical shifts (Figure S9).<sup>18,19</sup> Their relative  
26 configuration was unambiguously determined based on the observed <sup>3</sup>J<sub>HH</sub> and the key NOESY  
27 correlations (Figure 4c), assisted by molecular modelling employing 3D structural models  
28 generated after the reported X-ray structure of LNM E2 (Figure S9).<sup>20</sup> Finally, the absolute  
29 configurations at C-3, C-18 and the C $\alpha$  of the S-conjugated N-acetyl-cysteine (CysNAc) units  
30 were assigned to be the same as those found in LNM, L-Thr and mycothiol respectively, on the  
31 basis of biosynthetic and phylogenetic arguments later explained,<sup>7</sup> thus providing the full absolute  
32 stereochemistry of **1** and **2** (Figure 4a). Although chemical instability issues hampered a complete  
33 spectroscopic characterization of compounds corresponding to peaks **c** and **d** (Figure 3a),  
34 fortunately in the case of compound from peak **d**, named LRG A3 (**3**), it was possible at least to  
35 unequivocally assign C<sub>23</sub>H<sub>23</sub>ClN<sub>2</sub>O<sub>8</sub>S as its molecular formula (see Supporting Information).  
36 Based on this, its shared biosynthetic origin with **1** and **2** and the reported structure for LNM E4,<sup>20</sup>  
37 we have proposed a tentative chemical structure for **3** (Figure 4a).  
38  
39  
40  
41  
42  
43  
44  
45  
46  
47  
48  
49  
50  
51  
52  
53  
54  
55  
56  
57  
58  
59  
60



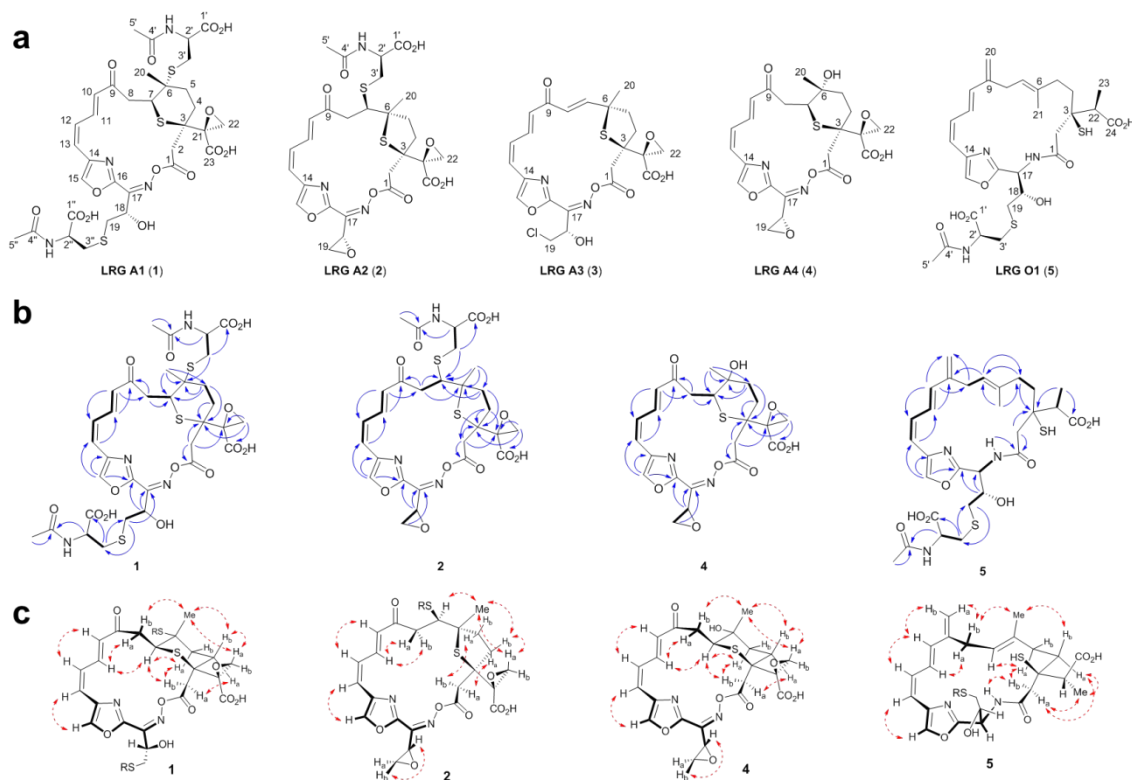


**Figure 4.** Structure of largymicins (LRGs). a) LRG A1 (1), A2 (2), A3 (3), A4 (4) and O1 (5). b) Key COSY correlations (bold bonds) and  $^1\text{H}$  to  $^{13}\text{C}$  HMBC correlations (blue arrows) determining the connectivity of LRGs. c) Key NOESY correlations (red arrows) employed alongside  $^3J_{\text{HH}}$  to determine the relative configuration of LRGs.

LRGs thus show some structural similarity to three analogs of LNM (Figure 1a).<sup>20</sup> As LNMs E2 and E3, **1** contains a tetrahydrothiopyran ring embedded within the macrocycle while **2** contains a macrocycle-embedded tetrahydrothiophene ring, as found in LNM E4. However, LRGs display unique structural features compared to known LNMs: (i) they contain a 19-membered macrolactone ring closed through an unprecedented oxime ester bond instead of an 18-membered macrolactam ring. Very interestingly, natural oxime esters have been described previously only in some vibrilactoximes of fungal origin,<sup>21</sup> and LRGs remarkably represent the first time that a macrocyclic natural product cyclized through an oxime ester is reported; (ii) they have an oxazole aromatic ring instead of a thiazole heterocycle; (iii) they contain one (in **2**) or two (in **1**) S-conjugated CysNAc moieties that are absent in LNMs; (iv) the C-3 side chain substituent contains an epoxide also absent in known LNMs; (v) the side chain at C-17 also differs from the displayed by known LNMs. Therefore, LRGs constitute a new group of oxazole-containing

1  
2  
3 169 macrocyclic oxime esters within the LNM family of natural products. Since cluster 11 was shown  
4 170 to encode LRGs it was renamed as cluster *Irg*.

5  
6 171 **Identification of *Irg* homologous BGCs in other strains. Characterization of LRG A4.**

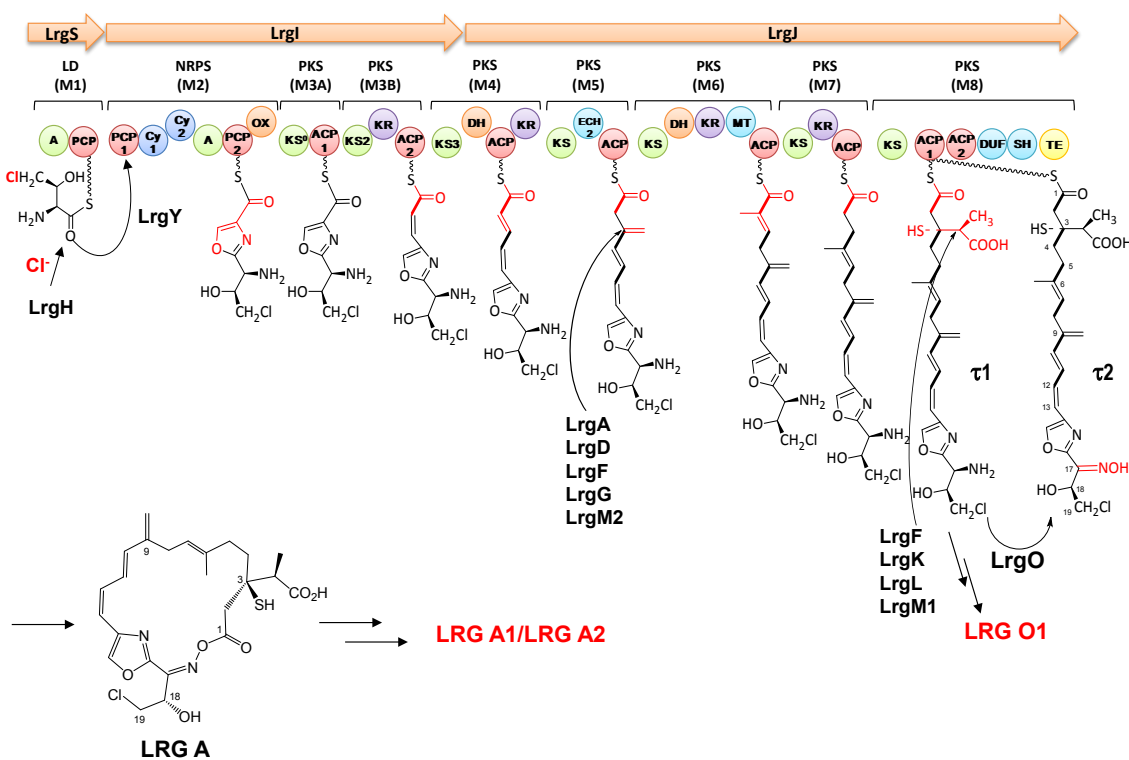
7  
8 172 Bioinformatics analysis of *Irg* gene products showed that Lrg proteins were highly similar (above  
9 173 85% identity) to proteins encoded by clusters *M1013* from *Streptomyces* M1013, *scan* from *S.*  
10 174 *canus* ATCC 12647, and also to a recently identified *CB01373* cluster in *Streptomyces* CB01373  
11 175 (Table 1).<sup>7</sup> All these clusters showed high synteny among them, being more remarkable that  
12 176 between *Irg* and clusters *M1013* and *scan* (Figure 2). Clusters *scan* and *CB01373* have been  
13 177 grouped into clade VII in a recent classification of LNM-type BGCs based on a phylogenetic  
14 178 analysis of the DUF-SH didomains.<sup>7</sup> According to these similarities, clusters *Irg* and *M1013*  
15 179 would constitute two new members of this clade. The phylogenetic classification of *Irg*  
16 180 automatically renders the C-3 absolute configuration of LRGs as being equal to that found for  
17 181 LNMs, since members of clade VII and clade I (to which the known LNMs producers belong)  
18 182 share the same stereochemistry at that chiral center.<sup>7</sup> Furthermore, members of clade VII are  
19 183 also predicted to select L-Thr as starting amino acid in the biosynthesis of their encoded  
20 184 compounds.<sup>7</sup> Since L-Thr is the precursor, as later explained, of the functional groups at C-18/C-  
21 185 19 observed in **1-3**, the absolute stereochemistry of C-18 in LRGs matches that of the  
22 186 hydroxylated methine in L-Thr.

23  
24 187 In order to determine if some of those strains also produce LRGs, *S. canus* was cultivated  
25 188 under the same conditions mentioned above. Since no LRG were detected, the activator *IrgR2*  
26 189 was overexpressed using pEM4ATc-R2. Production of LRGs by the resultant recombinant strain  
27 190 *S. canus* WT-R2 was readily detected (Figure 3b). The main compound produced by this strain  
28 191 (corresponding to peak **e** in Figure 3b) was isolated and named LRG A4 (**4**). The structure of **4**  
29 192 was determined (see Supporting Information) after extensive HRMS and 1D (<sup>1</sup>H) and 2D NMR  
30 193 analyses, likewise assisted by comparison with the NMR data of **1**, **2** and the reported for known  
31 194 LNMs. Its connectivity was established based on the determined molecular formula and the  
32 195 observed key correlations in the COSY and HMBC spectra (Figure 4b). The *Z* stereochemistry of  
33 196 the oxime double bond and the whole relative configuration were determined as described for **1**  
34 197 and **2** (Figures 4c and S8). Since the cluster *scan* and *Irg* belong to the same clade VII,<sup>7</sup> the  
35 198 absolute configurations of the chiral centers at C-3 and C-18 were assigned to be the same as **1**,  
36 199 thus providing the full absolute stereochemistry of **4** (Figure 4a).

37  
38 200 Discovery of LRG A4 confirmed that cluster *scan* also encodes LRGs and suggests that  
39 201 clusters *M1013* and *CB01373* most probably also direct the biosynthesis of LRGs in their  
40 202 corresponding strains.

203 **Limits of *Irg* biosynthesis gene cluster.** Except *IrgR4*, genes between *IrgT1* and *IrgC3* in the *Irg*  
 204 BGC are also preserved in *M1013* and *scan* clusters. Upstream *IrgT1* and downstream *IrgC3* this  
 205 homology is lost (Table 1 and Figure 2). Therefore, these two genes were tentatively proposed as  
 206 the limits of the *Irg* gene cluster. To confirm it, genes located at both ends of the cluster were  
 207 sequentially inactivated, followed by overexpressing *IrgR2* into the generated mutants (and also  
 208 into the  $\Delta IrgR3$  mutant mentioned above), and by analysis of LRGs production (see Supporting  
 209 Information). Strains with deletions in *orf18*, *IrgT1*, *IrgR3*, *IrgP1* and *orf52* still produced LRGs,  
 210 indicating that these genes were not essential for LRGs production in the tested conditions.  
 211 However, production of **2** was abolished in mutants  $\Delta IrgC1$ -R2 and  $\Delta IrgC3$ -R2, indicating that  
 212 *IrgC1* and *IrgC3* were essentials for LRGs production. According to these data and taking in  
 213 consideration that genes *IrgT1*, *IrgR3* and *IrgP1* are also conserved in *M1013*, *scan* and in  
 214 *CB01373* BGCs, we propose *IrgT1* as the left limit and *IrgC3* as the right limit of *Irg* BGC (Figure  
 215 2).

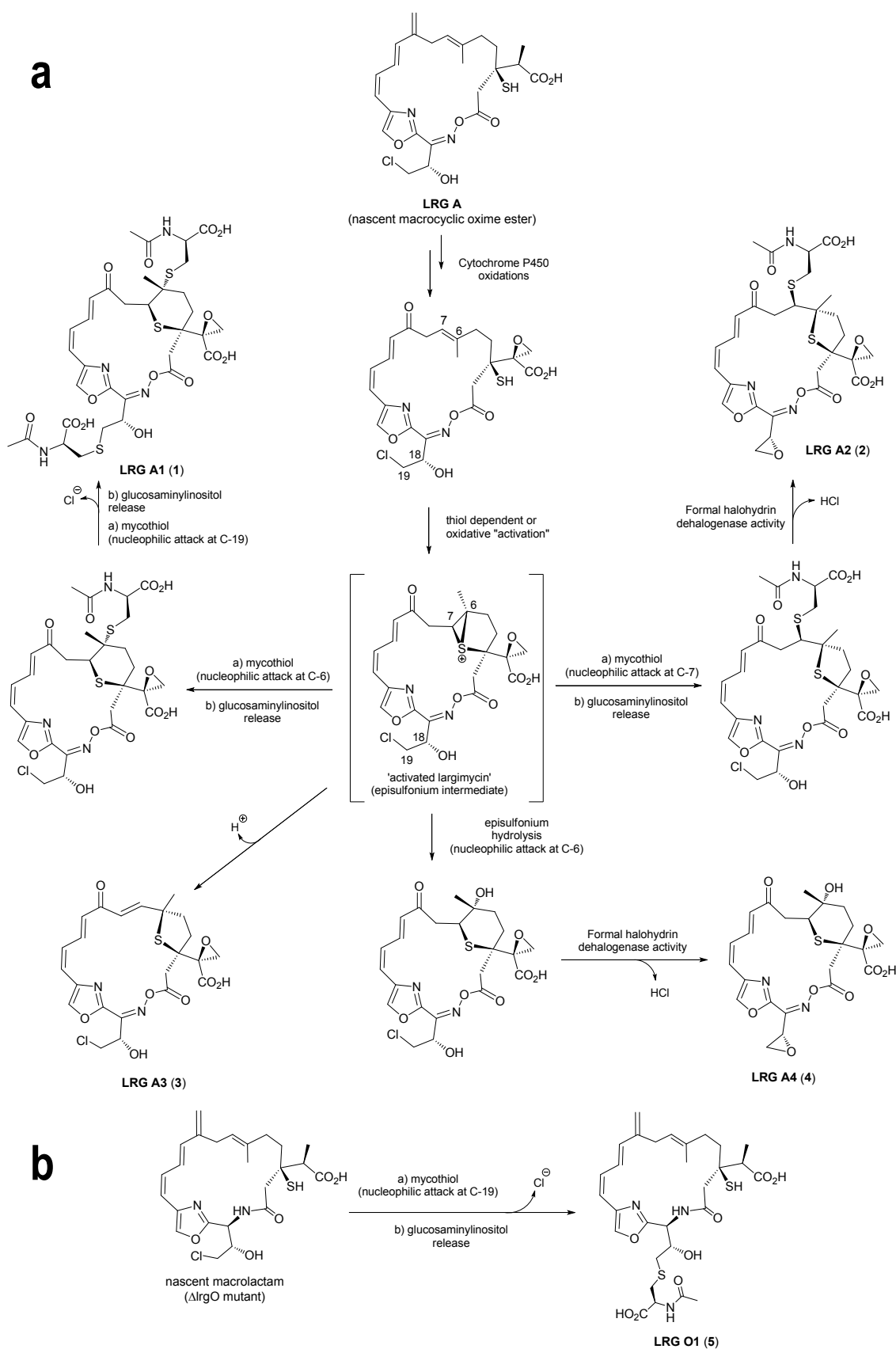
216 **Analysis of the largimycin biosynthetic gene cluster and proposed biosynthesis pathway.**  
 217 The *Irg* cluster spans 69.81 kb and encompasses thirty three genes (Figure 2, Table 1). Based on  
 218 the structure of LRGs and on bioinformatic analysis, a pathway for LRGs biosynthesis is  
 219 proposed (Figure 5).



220  
 221 **Figure 5.** Proposed biosynthesis pathway for largimycins.  
 222

1  
2  
3 223 The biosynthesis would start by synthesizing the peptide moiety by the NRPS LrgI. This NRPS  
4  
5 224 lacks a typical loading module. This role could be fulfilled by several discrete proteins (LrgS, LrgH  
6  
7 225 and LrgY) that show similarity to SyrB1, SyrB2 and SyrC respectively, from the syringomycin  
8  
9 226 BGC of *Pseudomonas syringae*.<sup>22</sup> LrgS is a didomain enzyme that contains an adenylation (A)  
10  
11 227 domain at the N-terminus and a peptidyl carrier protein (PCP) domain at the C-terminus. The  
12  
13 228 specificity-conferring codes for the A domain (DFWNVGMVH and  
14  
15 229 LQTHFDFSVWEGNQVFGGEVNMYGITETTVHVTA),<sup>23,24</sup> predict L-Thr as substrate and are  
16  
17 230 identical to those identified in WP\_059300325.1 and in CB01373\_Q from *scan* and *CB01373*  
18  
19 231 BGCs, respectively. That prediction was confirmed for CB01373\_Q by *in vitro* assays indicating  
20  
21 232 that members of clade VII,<sup>7</sup> which also includes LrgS, recognize L-Thr as substrate, a specificity  
22  
23 233 in agreement with the chemical structure of LRGs. LrgH shows similarity to nonheme Fe<sup>II</sup>  $\alpha$ -  
24  
25 234 ketoglutarate- and O<sub>2</sub>-dependent aliphatic halogenases such as SyrB2, which chlorinates L-Thr  
26  
27 235 tethered to the PCP domain of SyrB1.<sup>25</sup> LrgY is a member of the  $\alpha/\beta$ -hydrolase family to which  
28  
29 236 SyrC belongs, which shuttles L-threonyl/4-Cl-L-threonyl moieties *in trans* between the PCP  
30  
31 237 domain of SyrB1 and that located at the ninth module of SyrE NRPS.<sup>26</sup> According to these  
32  
33 238 similarities LrgSHY would constitute the loading module (Module 1) of NRPS LrgI (Figure 5): LrgS  
34  
35 239 would activate and load L-Thr; then, this amino acid tethered to the PCP domain of LrgS would be  
36  
37 240 halogenated by LrgH and transferred by LrgY to the hybrid NRPS/PKS LrgI. Although **1**, **2** and **4**  
38  
39 241 are not halogenated compounds, they contain a CysNAc-S-conjugate substituent at C-19 (**1**) or  
40  
41 242 an epoxide at C-18/C-19 (**2** and **4**), which most likely derive from the corresponding halohydrin  
42  
43 243 motif of the 4-Cl-L-threonyl precursor unit in the biosynthesis (Figure 6).  
44  
45 244 The identified molecular formula for **3** (C<sub>23</sub>H<sub>23</sub>ClN<sub>2</sub>O<sub>8</sub>S) indeed provides a direct evidence for  
46  
47 245 halogenation during LRGs biosynthesis. Since **2** and **4** do not contain a chlorine atom but the  
48  
49 246 chlorination of the tethered L-Thr is apparently required for the formation of the epoxide functional  
50  
51 247 group observed in the starting amino acid unit, the halogenation event may be considered  
52  
53 248 'cryptic' within the overall biosynthetic pathway leading to these LRGs. Such a biosynthetic route  
54  
55 249 resembles the reported 'cryptic' chlorination step catalyzed by the halogenase CmaB in the  
56  
57 250 coronatine biosynthesis pathway, which is required for the formation of the cyclopropyl ring  
58  
59 251 observed in the non-chlorinated isolated compound.<sup>27</sup> Several other BGCs related to *Inm* BGC  
60  
252 and grouped into clades IV, V, VIII, XIV, XV and XVIII,<sup>7</sup> also encode a SyrB1, SyrB2 and SyrC  
253 like proteins, which could fulfill the same roles in their respective pathways than those herein  
254 proposed for LrgSHY.

255 The N-terminus of LrgI corresponds to a NRPS (Module 2, Figure 5). It contains a domain



256

257 **Figure 6. a)** Proposed biosynthetic origin of S-conjugated N-acetyl-cysteine moieties and C-18/C-  
 258 19 oxirane rings in largimycins involving the key episulfonium intermediate; b) Proposed  
 259 biosynthetic origin of LRG O1.

1  
2  
3 260 organization (PCP1-Cy1-Cy2-A-PCP2-Ox) with two-tandem cyclization (Cy) and one oxidation  
4 261 (Ox) domain, found in some modules involved in thiazole and oxazole ring formation, such as the  
5 262 hybrid NRPS/AT-less Type I PKSs of *Inm*-type gene clusters.<sup>7</sup> Cy domains are responsible for the  
6 263 condensation, cyclization and dehydration events that lead to the formation of thiazoline and  
7 264 oxazoline rings. Tandem Cy domains are found in some NRPS such as the VibF from vibriobactin  
8 265 BGC, Cy2 carrying out the condensation step and Cy1 doing the cyclization/dehydration steps.<sup>28</sup>  
9 266 Ox domains catalyze the oxidation of thiazoline- and oxazoline-S-enzyme intermediates into the  
10 267 corresponding thiazole- and oxazole-S-enzymes.<sup>29</sup> The presence of this Ox domain in LrgI is  
11 268 consistent with the oxazol ring found in LRGs. The substrate specificity-conferring codes of LrgI A  
12 269 domain do not match any known A domain, but it is more similar to those recognizing L-Cys in  
13 270 Lnml and in other *Inm*-type BGCs. Noticeable, the LrgI A domain and its homologous  
14 271 counterparts in *scan*, *M1013*, and *CB01373* BGCs, share identical codes containing conserved  
15 272 amino acids that differ from those recognizing L-Cys (Table S2). Given the chemical structure of  
16 273 LRGs, the oxazole ring would be synthesized by the condensation of Thr and Ser residues.  
17 274 According to this, we propose that the A domains of LrgI and WP\_059300322.1 from *scan* would  
18 275 specify for Ser.

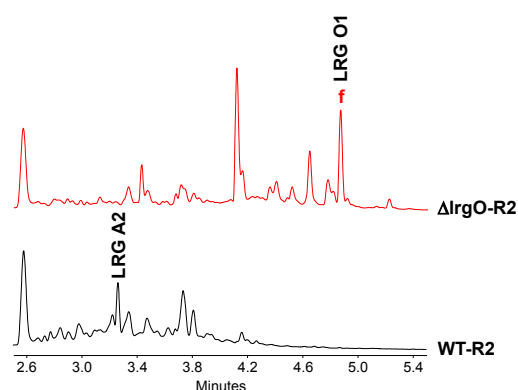
19 276 The C-terminus of LrgI corresponds to an AT-less Type I PKS. This together with the AT-less  
20 277 Type I PKS LrgJ would constitute the PKS megasynthase responsible for the biosynthesis of the  
21 278 PK chain of LRGs. This PKS is organized into six modules (Figure 5): LrgI contains Modules 3A  
22 279 and 3B, and the  $\beta$ -ketoacyl synthase (KS) domain of Module 4 that is splitted between LrgI and  
23 280 LrgJ; LrgJ also contains Modules 5 to 8. The PKS LrgI shows a domain organization similar to  
24 281 Lnml from *Inm* BGC:<sup>15</sup> KS1-Acyl Carrier Protein (ACP)1-KS2-Ketoreductase (KR)-ACP2-KS3.  
25 282 KS2 and KS3 contain the canonical catalytic triad CHH that is necessary for decarboxylative  
26 283 condensation,<sup>30</sup> but KS1 has a mutated triad (CAH). In Lnml both KS1 and KS2 domains are  
27 284 essential for LNM biosynthesis but playing different roles: KS1 transfers the PCP-tethered  
28 285 peptidyl intermediate of NRPS Module 2 to the ACP1 of PKS Module 3, and KS2 catalyzes the  
29 286 decarboxylative condensation event between peptidyl-S-ACP1 and malonyl-S-ACP2.<sup>31</sup> Therefore,  
30 287 KS1-like domains correspond to domains in non-elongating modules, which are frequently found  
31 288 in AT-less Type I PKSs.<sup>32</sup> According to this, KS1 (renamed KS<sup>0</sup>)-ACP1 of LrgI would constitute a  
32 289 non-elongating module (Module 3A), while KS2-KR-ACP2 would be the first elongating module  
33 290 (Module 3B) for LRGs PK biosynthesis (Figure 5). Like Lnml,<sup>15</sup> Module 3B of LrgI also lacks a  
34 291 Dehydratase (DH) domain that would be required for double bond formation between C-12 and  
35 292 C-13.

1  
2  
3 293 The AT-less Type I PKS LrgJ shows the following domain composition (Figure 5): Module 4  
4 (DH-ACP-KR; the corresponding KS domain KS3 is located at LrgI), Module 5 (KS-ECH2-ACP),  
5 294  
6 Module 6 (KS-DH-KR-MT-ACP), Module 7 (KS-KR-ACP) and Module 8 (KS-ACP1-ACP2-DUF-  
7 295  
8 SH-TE). This organization is identical to that of PKS GnmT from the guanranmycin BGC,<sup>7</sup> but  
9 296  
10 297 differs from that of LnmJ at Modules 5 to 7:<sup>15</sup> LrgJ lacks the ACP1 domain at Module 6, the DH  
11 298  
12 domain at Module 7 and it contains an Enoyl-CoA hydratase (ECH2) domain at Module 5.  
13 299  
14 Members of the ECH2 family of enzymes catalyze a decarboxylation step to afford a  $\beta$ -alkylating  
15 300  
16 intermediate during incorporation of  $\beta$ -branch groups to natural products.<sup>32,33</sup> They can exist as  
17 301  
18 freestanding proteins or can be located as domains within larger multidomain proteins as it occurs  
19 302  
20 in GnmT and LrgJ. The existence of this ECH2 domain at Module 5 together with the presence of  
21 303  
22 genes for so called “HMG cassettes” (see below) in the *lrg* BGC suggests the incorporation of an  
23 304  
24 olefinic exomethylene group at C-9 during the biosynthesis of LRGs. Module 6 contains a  
25 305  
26 methyltransferase (MT) domain, which agrees with the presence of a methyl group substituent at  
27 306  
28 C-6 in LRGs. Like all *Inm*-like BGCs, Module 8 contains a KS, two tandem ACP domains, a DUF  
29 307  
30 domain, a SH domain and a thioesterase domain (TE). Runs of ACP domains are often found in  
31 308  
32 modules involved in  $\beta$ -alkylation and are supposed to be an anchor point for the “HMG proteins”  
33 309  
34 that are responsible for introducing a  $\beta$ -branch.<sup>33</sup> In a similar way as in LNM biosynthesis,<sup>6</sup>  $\beta$ -  
35 310  
36 alkylation should occur at the C-3 position of the  $\beta$ -ketoacyl-S-ACP intermediate attached to  
37 311  
38 Module 8 of LrgJ, and before the installation of the SH group by DUF-SH domains. These DUF-  
39 312  
40 SH didomains are present in all BGCs for LNM family of compounds identified so far,<sup>7</sup> and are  
41 313  
42 involved in sulfur incorporation into the PK backbone: the DUF domain adding L-Cys to the PK,  
43 314  
44 and the SH domain catalyzing the C-S bond cleavage that originates the C-3 sulfur.<sup>6</sup>  
45 315  
46 Phylogenetic analyses of DUF and SH domains from *Inm*-like BGCs showed they tend to cluster  
47 316  
48 into two groups: one from pathways that use propionyl-S-ACP as the predicted substrate and the  
49 317  
50 other from pathways using acetyl-S-ACP.<sup>7</sup> The LrgJ-DUF-SH didomain is more similar to those  
51 318  
52 that putatively use propionyl-S-ACP as substrate, which is in accordance with the alkyl branch at  
53 319  
54 C-3 displayed by LRGs. As already mentioned, the DUF-SH didomain in the *lrg* gene cluster is  
55 320  
56 phylogenetically classified in clade VII, the same as the homologous didomains in the *scan* and  
57 321  
58 *CB01373* clusters,<sup>7</sup> automatically indicating that LRGs and LNMs share the same absolute  
59 322  
60 stereochemistry at C-3 since sulfur incorporation proceeds in both clades I (LNMs) and VII  
323 (LRGs) with the same stereoselectivity.

324 Biosynthesis of the PK chain requires an AT in each elongation step. However, neither LrgI  
325 nor LrgJ contain AT domains (AT-less PKSs). This function would be fulfilled by LrgG that shows  
326 high similarity to the *trans*-AT LnmG from LNM pathway and is predicted to accept malonyl-CoA

1  
2  
3 327 as substrate,<sup>34</sup> in agreement with the chemical structure of LRGs. The *lrg* BGC also contains a  
4  
5 328 phosphopantetheinyl transferase encoding gene (*lrgQ*) that could be involved in transferring 4'-  
6  
7 329 phosphopanteteine to ACPs of PKS and to PCPs of NRPS,<sup>35</sup> and a Type II TE (*lrgN*) that could  
8  
9 330 play an editing role eliminating aberrant growing chains from the PKS.<sup>36</sup>

10 331 Considering all information mentioned above and taking into account the chemical structure of  
11  
12 332 LRGs, a putative tethered full-length peptide-PK intermediate  $\tau$ 1 would result from the action of  
13  
14 333 LrgSHYGIJ, "HMG proteins" (see below) and some enzymatic activities required to generate a  
15  
16 334 C12-C13 Z double bond and to generate a methylene at C-5. All *lrm*-like BGCs contain a Module  
17  
18 335 3B that also lack the DH domain, but even so all LNM-like compounds described so far show the  
19  
20 336 C12-C13 Z double bond. Formation of the fully saturated ethylene unit corresponding to the C4-  
21  
22 337 C5 bond would require the existence of a DH and an enoyl reductase (ER) domain at Module 7 of  
23  
24 338 LrgJ, which are missing (Figure 5). Interestingly, GNMs also contain a saturated ethylene unit at  
25  
26 339 those positions and similarly to LrgJ the corresponding module also lacks DH and ER domains.<sup>7</sup>  
27  
28 340 Therefore, some of these functions could be supplied by the action of domains at other modules  
29  
30 341 or provided *in trans* by unknown enzymes. Both features have been described in other AT-less  
31  
32 342 PKs.<sup>32</sup> Formation of the tethered intermediate  $\tau$ 2 would be followed by its release through a  
33  
34 343 cyclization, catalyzed by the TE domain of Module 8 of LrgJ, via an unprecedented ester bond  
35  
36 344 involving the oxime hydroxy group, generating the putative nascent macrolactone intermediate  
37  
38 345 LRG A (Figure 5). This cyclization would require a previous conversion of the amino terminal  
39  
40 346 group of  $\tau$ 1 into an oxime group to render the putative intermediate  $\tau$ 2. The *lrg* cluster contains  
41  
42 347 *lrgO* that encodes a putative NAD(P)/FAD-dependent oxidoreductase similar to CImM (44%  
43  
44 348 identical amino acids) from the the collismycin BGC,<sup>37</sup> which is involved in the formation of an  
45  
46 349 oxime functional group. To determine if LrgO plays a similar role in the formation of the oxime  
47  
48 350 group of LRGs, its coding gene was inactivated (see Supporting Information). After expressing  
49  
50 351 *lrgR2* into this mutant, cultivation of the resultant strain ( $\Delta$ lrgO-R2) showed that previous LRGs  
51  
52 352 production was abolished and some new peaks were detected (Figure 7).



353



1  
2  
3 354 **Figure 7.** Production of largimycins by *S. argillaceus*  $\Delta$ lrgO. UPLC chromatograms (300 nm) of  
4 ethyl acetate extracts of *S. argillaceus* WT-R2 and *S. argillaceus*  $\Delta$ lrgO-R2 strains cultivated in  
5 SM30a. Peaks for LRG A2 and LRG O1 are indicated.  
6  
7  
8  
9

10 357  
11 358 Compound from peak **f** was purified and chemically characterized. It corresponds to a novel  
12 359 compound named LRG O1 (**5**) (Figure 4a). The structure of **5** was likewise determined (see  
13 360 Supporting Information) after detailed HRMS and NMR spectroscopic analyses, further assisted  
14 361 by comparisons with the NMR data of **1**, **2**, **4**, LNM E1 and GNM B.<sup>7,20</sup> Its connectivity was  
15 362 derived from the determined molecular formula and the observed key correlations in the COSY  
16 363 and HMBC spectra (Figure 4b), while determination of the relative configuration relied on  
17 364 molecular modeling combined with analysis of the observed  $^3J_{\text{HH}}$  and the key NOESY correlations  
18 365 (Figures 4c and S8). Based on its shared biosynthetic origin, the absolute configuration at C-3  
19 366 and C-18 were assigned to be the same as **1**, while the membership of cluster *lrg* to the  
20 367 mentioned clade VII,<sup>7</sup> also allows assigning to C-22 the same absolute configuration determined  
21 368 for LNM E1,<sup>20</sup> and to C-17 the same stereochemistry as the  $\alpha$  position of L-Thr, thus providing  
22 369 the full absolute stereochemistry of **5** (Figure 4a). Interestingly, **5** lacks the ketone at C-9  
23 370 observed for **1-4** but rather displays an olefinic exomethylene group at that position, as described  
24 371 for GNMs and WSMS,<sup>7</sup> confirming the incorporation of this moiety during PK biosynthesis.  
25 372 Additionally, **5** also lacks the oxime functional group observed in **1-4**, thus being a macrolactam  
26 373 as are the known LNMs, GNMs and WSMS. This structural feature contrasts with the oxime ester  
27 374 closing of the macrocycle in **1-4** and ultimately demonstrates the essential role of LrgO in the  
28 375 oxidation of the amine group of the starting amino acid unit to render the oxime. Such oxidation  
29 376 before offloading the fully assembled tethered intermediate  $\tau$ 2 by macrocyclization forming the  
30 377 oxime ester (Figure 5) resembles the case of the giant stambomycin macrolides,<sup>38</sup> where a  
31 378 cytochrome P450-catalyzed hydroxylation of the PK tethered chain is required for its release by  
32 379 macrolactonization in what was claimed to be a novel mechanism for macrolactone formation in  
33 380 PK antibiotic biosynthesis. In the case of **1-4** we are likewise dealing with a novel mechanism in  
34 381 secondary metabolism for offloading linear tethered precursors by macrocyclization via oxime  
35 382 ester formation. However, the macrolactam nature of **5** demonstrates that amine oxidation is not  
36 383 essential for successful LRG offloading by macrocyclization, as otherwise expected based on the  
37 384 structure of known LNMs. The structure of **5** (Figure 4a) is closely related to LNM E1 and GNM B  
38 385 (Figure 1),<sup>7,20</sup> being very similar to LRG A, the proposed nascent macrocyclic oxime ester  
39 386 intermediate of the LRG pathway (Figure 5).  
40  
41  
42  
43  
44  
45  
46  
47  
48  
49  
50  
51  
52  
53  
54  
55  
56  
57  
58  
59  
60

1  
2  
3 387 Domain organization of Modules 5 and 8 suggests the incorporation of  $\beta$ -branches at C-9 and  
4 C-3 during PK elongation (Figure 5).  $\beta$ -branching requires a dedicated set of enzymes (“HMG  
5 388 cassettes”) typically constituted by an ACP, an AT, a KS and a hydroxymethylglutaryl-CoA  
6 389 cassettes”) typically constituted by an ACP, an AT, a KS and a hydroxymethylglutaryl-CoA  
7  
8 390 synthase (HCS), which introduce a  $\beta$ -branch into the growing PK chain that can be further  
9  
10 391 dehydrated and decarboxylated by ECH proteins/domains.<sup>33,39</sup> The *Irg* BGC contains genes  
11  
12 392 coding for discrete ACPs (*IrgL* and *IrgA*) and KS (*IrgD*), HCSs (*IrgM1* and *IrgM2*), a dehydratase  
13  
14 393 ECH1 (*IrgF*) and a bifunctional AT/decarboxylase (DC) (*IrgK*) (Table 1). In addition, there is an  
15  
16 394 ECH2 domain at Module 5. LrgKLM1 and LrgF are homologous to LnmKLM and LnmF  
17  
18 395 respectively, from the *Inm* BGC,<sup>15</sup> which have been shown to participate in the attachment of a  
19  
20 396 propionyl branch at C-3 during LNM biosynthesis.<sup>5</sup> A similar role could be fulfilled by LrgKLM1  
21  
22 397 and LrgF in the biosynthesis and attachment of the  $\beta$ -alkyl branch at C-3 of LRGs (Figure 5). The  
23  
24 398 existence of additional genes encoding HCS (LrgM2), ACP (LrgA) and KS (LrgD) proteins,  
25  
26 399 together with the presence of the ECH2 domain at Module 5, suggests the incorporation of an  
27  
28 400 olefinic exomethylene group at C-9 (Figure 5). That group is present in **5** (Figure 4a). Intriguingly,  
29  
30 401 **1** and **2** contain a keto group at that position, which suggests that the olefinic exomethylene group  
31  
32 402 is modified after being incorporated to the PK chain and that the introduction of this group is a  
33  
34 403 “cryptic” step in the biosynthetic pathway.

35  
36 404 Several biosynthesis steps should occur between the putative nascent oxime macrolactone  
37  
38 405 intermediate LRG A and the final compounds **1** and **2** (Figure 5). The main differences between **1**  
39  
40 406 and **2** and the proposed nascent intermediate LRG A are the existence of a saturated single bond  
41  
42 407 between C-6 and C-7; a keto group at C-9; an epoxide at the C-3 branch; a C-17 side chain  
43  
44 408 containing an S-conjugated CysNAc moiety (**1**) or an epoxide (**2**); a tetrahydrothiopyran ring  
45  
46 409 system between C-3 and C-7 (in **1**) or a tetrahydrothiophene heterocycle between C-3 and C-6  
47  
48 410 (**2**); and one CysNAc-S-conjugate substituent at C-6 (**1**) or at C-7 (**2**) (Figure 3a). Three  
49  
50 411 cytochromes P450 encoding genes (*IrgC1*, *IrgC2* and *IrgC3*), identified within *Irg* cluster (Figure 2,  
51  
52 412 Table 1), could be involved in epoxide formation at the C-3 side chain and in the conversion of  
53  
54 413 the exomethylene group at C-9 into a keto group. Both epoxidation and dealkylation reactions  
55  
56 414 have been shown to be carried out by cytochrome P450s.<sup>40</sup> In this work we have shown that  
57  
58 415 *IrgC1* and *IrgC3* are required for LRGs biosynthesis (see above). The reported isolation of WSM  
59  
60 416 A3, which contains an epoxide at C-9/C-22, alongside WSMs A1 and A2, which display an  
417 olefinic double bond at those positions,<sup>7</sup> suggests a possible oxidative dealkylation mechanism  
418 involving a first epoxidation step to explain the conversion of the olefinic exomethylene at C-9 into  
419 the corresponding ketone observed in **1**, **2** and **4**.

1  
2  
3 420 There are several genes (*lrgE*, *lrgP2*, *lrgW1*, *lrgW2*, *lrgX* and *lrgZ*) that have homolog  
4 421 counterparts in *Inm* BGC and related clusters, and some others (*lrgB* and *lrgP1*) that do not have  
5 422 homologs in *Inm* BGC but they are conserved in several *Inm*-type BGCs, including those for GNM  
6 423 and WSM biosynthesis.<sup>7</sup> This suggests that the encoded proteins might play common functions in  
7 424 the biosynthesis of this family of compounds. All of these *Inm* homologous genes have been  
8 425 shown to be essential for LNM production,<sup>15</sup> but only in the case of LnmE a possible role has  
9 426 been proposed in sulfur incorporation required to form the 1,3-dioxo-1,2-dithiolane moiety of  
10 427 LNM.<sup>20</sup> We have shown that inactivation of *lrgP1* does not affect LRG production (see above). It  
11 428 is tempting to propose that all or some of these genes might contribute to the formation of **1** and  
12 429 **2**, which could thus be envisaged deriving from LRG A via an oxidative mechanism involving a  
13 430 putative episulfonium ion intermediate, in analogy to LNM and LNM E1 as already also proposed  
14 431 for WSMs (Figure 6).<sup>7,20</sup>

15 432 LRGs **1** and **2** contain two and one S-conjugated CysNAc moieties, respectively. On the one  
16 433 hand, the CysNAc-S-conjugate substituent observed at C-6 or C-7 is proposed to be incorporated  
17 434 by nucleophilic attack of the CysNAc thiol group, from a mycothiol molecule, over those carbons  
18 435 (C-6 for **1** and C-7 for **2**) in the putative episulfonium ion intermediate derived from the nascent  
19 436 LRG A by an oxidation process (Figure 6). On the other hand, the CysNAc-S-conjugate  
20 437 substituent observed at C-19 in **1** and in **5** is proposed to be incorporated by nucleophilic attack of  
21 438 the same thiol group over the chlorinated C-19 in the halohydrin functionality of the starting 4-Cl-  
22 439 L-Thr unit (Figure 6). Thus, these LRGs would be shunt products generated by non-enzymatic  
23 440 events based on the inherent nucleophilicity of thiols, as it has been proposed for the  
24 441 biosynthesis of other compounds containing S-conjugated CysNAc adducts,<sup>12,41</sup> and could be  
25 442 considered derived from a LRG detoxification mechanism based on CysNAc S-alkylation by the  
26 443 episulfonium intermediate. This would provide an alternative mechanism for self-immunity in  
27 444 actinomycete producers of natural products of the LNM family additional to the inherent self-  
28 445 resistance based on the prodrug nature of LNM itself, claimed to be reductively activated in the  
29 446 presence of thiols after cellular uptake.<sup>42</sup> As suggested by Maier et al. (2014),<sup>41</sup> S-conjugated  
30 447 CysNAc most probably originates from mycothiol, the major low molecular weight thiol in  
31 448 actinomycetes, which plays important antioxidant and detoxification roles in these  
32 449 microorganisms.<sup>43,44</sup> After mycothiol conjugation with the corresponding metabolite precursor  
33 450 (episulfonium and chlorinated LRG), the amide bond between the cysteine and the GlcNAc  
34 451 moieties of mycothiol would be hydrolyzed by the action of a specialized amidase (Mca)  
35 452 releasing the corresponding mercapturic acids, the CysNAc-S-conjugated metabolites (**1**, **2**), plus  
36 453 glucosaminylinositol which is recycled for further mycothiol biosynthesis (Figures 6 and S9). This

1  
2  
3 454 biosynthetic origin of the CysNAc moieties automatically establishes the L absolute configuration  
4  
5 455 at C<sub>α</sub> of these amino acid units. Interestingly, the absence of any S-conjugated CysNAc  
6  
7 456 substituent in **4**, the main largimycin produced by *S. canus*, suggests that the inherent cellular  
8  
9 457 levels of mycothiol are much higher in *S. argillaceus*, something compatible with the variability of  
10  
11 458 mycothiol content among actinomycetes.<sup>44</sup>

12 459 Bearing in mind the cryptic halogenation step of the tethered L-Thr starting unit catalyzed by  
13  
14 460 the action of the LrgH halogenase, it can be proposed that formally a halohydrin dehalogenase  
15  
16 461 enzymatic activity is responsible for the formation of the oxirane ring at C-18/C-19 observed in **2**  
17  
18 462 and **4**. However, known halohydrin dehalogenases are examples of postindustrial evolution of  
19  
20 463 bacterial enzymes to acquire activity toward the degradation of halogenated xenobiotics.<sup>45</sup> As  
21  
22 464 expected, no homolog of halohydrin dehalogenases was found either in the *lrg* cluster nor  
23  
24 465 elsewhere in *S. argillaceus* genome. Thus, the discovery of these oxirane-containing LRGs  
25  
26 466 reveals an unprecedented type of halohydrin dehalogenase activity herein proposed for first time  
27  
28 467 in secondary metabolite biosynthesis. The enzyme responsible must catalyze the formation of the  
29  
30 468 epoxide by a mechanism formally equivalent, from the point of view of the substrate, to that of  
31  
32 469 actual halohydrin dehalogenases but likely involving different type and arrangement of key  
33  
34 470 residues for interaction with the halohydrin motif and deprotonation of the halohydrin hydroxyl  
35  
36 471 group. At this stage, it cannot be defined whether such an enzyme acts over a tethered linear  
37  
38 472 precursor or over released chlorinated macrocycles. However, the isolation of **1** and **5**,  
39  
40 473 containing S-conjugated CysNAc at C-19, strongly suggests a freestanding chlorinated  
41  
42 474 macrocycle as the most probable substrate. Future identification of the gene involved in the  
43  
44 475 formation of the oxirane ring from its halohydrin precursor will provide very valuable information  
45  
46 476 and the access to eventual investigations on the biotechnological potential of a new kind of  
47  
48 477 halohydrin dehalogenase activity.

49 478

## 50 479 **CONCLUSION**

51 480 Largimycins, encoded by the silent *lrg* gene cluster in *S. argillaceus* and the homologous cryptic  
52  
53 481 *scan* cluster in *S. canus*, are new and structurally unique members of the leinamycin family of  
54  
55 482 natural products. These secondary metabolites contain an oxazol ring rather than the thiazole  
56  
57 483 found in known LNMs and they are also the first naturally occurring macrocycles closed via an  
58  
59 484 oxime ester bond ever reported. The flavin-dependent oxidoreductase LrgO responsible for the  
60  
61 485 formation of the oxime group through which macrocyclization in LRGs takes place has been  
62  
63 486 successfully identified shedding light on an unprecedented mechanism in secondary metabolism  
64  
65 487 for offloading linear tethered precursors by oxime ester based macrocyclization. Very

1  
2  
3 488 interestingly, the proposed biosynthesis of LRGs involves two cryptic steps: i) chlorination of L-  
4 489 Thr by the NRPS loading module and ii) incorporation of an olefinic exomethylene in the growing  
5 490 PK chain. The oxirane ring observed in the starting amino acid unit of LRGs is proposed to be  
6 491 derived from a formal halohydrin dehalogenase activity over the cryptic 4-Cl-L-Thr moiety which  
7 492 remarkably represents the first time that such enzymatic transformation is proposed in secondary  
8 493 metabolism. Future work will be required to identify the intriguing protein displaying such formal  
9 494 halohydrin dehalogenase activity. That enzyme and the oxime forming *N*-oxidase LrgO herein  
10 495 identified deserve, in our view, further exploration based on a possible potential as biocatalysts.  
11 496 The discovery of cryptic LRGs reveals novel and creative biosynthetic avenues employed by  
12 497 Nature to enrich the structural diversity of the LNM family of natural products and provides  
13 498 exciting genes which expand the toolbox to generate new 'non-natural' analogues by  
14 499 combinatorial biosynthesis which would be very valuable to further investigate structure-activity  
15 500 relationship in the fascinating LNM family.

501

## 502 **ASSOCIATED CONTENT**

### 503 **Supporting Information**

504 This material is available free of charge via the internet.

505 Strains, culture conditions, plasmids and DNA manipulations; Generation of mutants; Plasmid  
506 constructs for gene expression; UPLC Analysis and Purification of largimycins; Spectroscopic  
507 analysis of largimycins and molecular modelling; Structure elucidation of largimycins; Alignments  
508 of Lrg proteins with Lnm and Syr proteins; Confirmation of *Streptomyces argillaceus* mutants;  
509 UPLC analysis of *S. argillaceus* WT-R2 cultivated in different media; UPLC analyses of extracts  
510 from *S. argillaceus* mutants; Spectroscopic data of LRG A1-A4 and LRG O1; Energy-minimized  
511 molecular models of LRG A1-A4 and LRG O1; Determination of the oxime double bond  
512 stereochemistry; Mechanism of formation of a CysNAc-S-conjugate after nucleophilic attack of  
513 mycothiol over an alkyl chloride; Oligonucleotides used for PCR; Comparison of specificity-  
514 conferring codes of adenilation domains of hybrid NRPS/PKS from leinamycin (*Inm*)-type gene  
515 clusters; <sup>1</sup>H NMR and <sup>13</sup>C NMR data of LRG A1, LRG A2, LRG A4 and LRG O1.

### 516 **Accession Codes**

517 The sequence of *Streptomyces argillaceus lrg* gene cluster has been deposited at European  
518 Nucleotide Archive (EBI-ENA) under the accession number LR131959.1 and at MIBiG under the  
519 accession number BGC0001853.

520

## 521 **AUTHOR INFORMATION**

1  
2  
3 522 **Corresponding author**

4  
5 523 \*E-mail: [cmendezf@uniovi.es](mailto:cmendezf@uniovi.es)

6  
7 524

8 525 **ORCID**

9  
10 526 Carmen Méndez: 0000-0003-2729-841X

11  
12 527 Ignacio Pérez-Victoria: 0000-0002-4556-688X

13  
14 528 Jesús Martín: 0000-0001-7487-2790

15  
16 529 Fernando Reyes: 0000-0003-1607-5106

17  
18 530

19 531 **AUTHOR CONTRIBUTIONS**

20 532 C.M. and J.A.S. conceived and designed the project; A.B. and S.Y., conducted experiments; A.B.  
21  
22 533 and A.F.B. carried out compound purifications; I.P.V., J.M. and F.R. performed chemical  
23  
24 534 characterization of compounds; C.M. wrote the manuscript and I.P.V. contributed to preparing the  
25  
26 535 final version of it. All authors read and approved the final version of the manuscript.

27  
28 536

29 537 **Notes**

30 538 The authors declare no competing financial interest.

31  
32  
33 539

34 540 **ACKNOWLEDGMENTS**

35  
36 541 This work was supported by grants from the Spanish Ministry of Economy and Competitiveness,  
37  
38 542 MINECO (Grants BIO2014-56752-R and PIM2010EEI-00752 to C.M.), and by the grant “Apoyo a  
39  
40 543 grupos de excelencia”, Principado de Asturias-FEDER (FC-15-GRUPIN14-014). A.B. and S.Y.  
41  
42 544 were recipient of predoctoral fellowships from MINECO. The NMR spectrometer used in this work  
43  
44 545 was purchased via a grant for scientific and technological infrastructure from the Ministerio de  
45  
46 546 Ciencia e Innovación (PCT-010000-2010-4). We thank C. Olano for helping in managing DNA  
47  
48 547 sequences.

49  
50 548

51 549 **REFERENCES**

- 52 550 (1) Newman, D.J. and Cragg, G.M. (2016). Natural products as sources of new drugs from 1981  
53 551 to 2014. *J. Nat. Prod.* 79, 629–661.
- 54  
55 552 (2) Hara, M., Asano, K., Kawamoto, I., Takiguchi, T., Katsumata, S., Takahashi, K., and  
56  
57 553 Nakano, H. (1989). Leinamycin, a new antitumor antibiotic from *Streptomyces*: producing  
58  
59 554 organism, fermentation and isolation. *J. Antibiot. (Tokyo)* 42, 1768-17674.

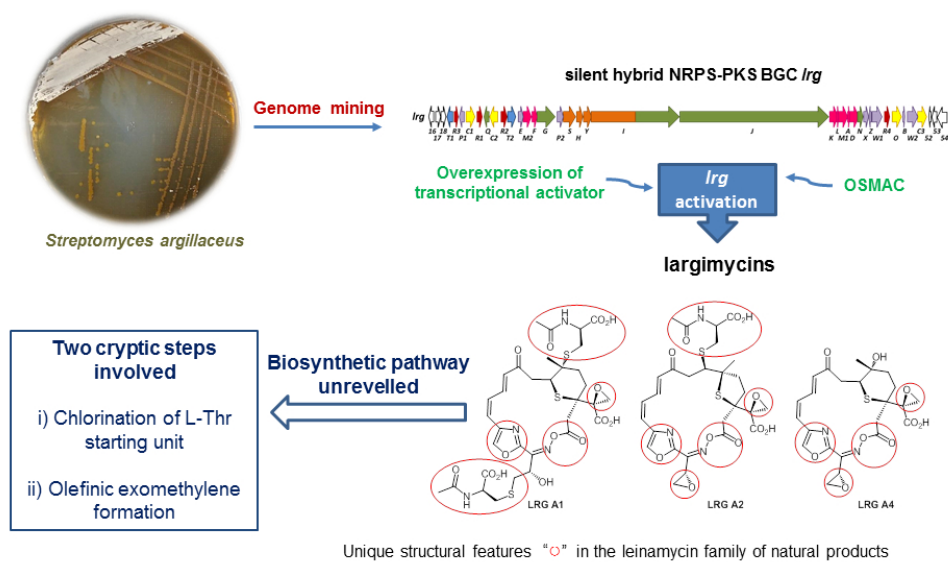
- 1  
2  
3 555 (3) Viswesh, V., Gates, K., and Sun, D. (2010). Characterization of DNA damage induced by a  
4 556 natural product antitumor antibiotic leinamycin in human cancer cells. *Chem. Res, Toxicol.*  
5 557 23, 99-107.  
6  
7  
8 558 (4) Cheng, Y.Q., Tang, G.L., and Shen, B. (2003). Type I polyketide synthase requiring a  
9 559 discrete acyltransferase for polyketide biosynthesis. *Proc. Natl. Acad. Sci. U. S. A.* 100,  
10 560 3149-3154.  
11  
12  
13 561 (5) Huang, Y., Huang, S.X., Ju, J., Tang, G., Liu, T., and Shen, B. (2011). Characterization of  
14 562 the *InmKLM* genes unveiling key intermediates for  $\beta$ -alkylation in leinamycin biosynthesis.  
15 563 *Org. Lett.* 13, 498-501.  
16  
17  
18 564 (6) Ma, M., Lohman, J.R., Liu, T., and Shen, B. (2015). C-S bond cleavage by a polyketide  
19 565 synthase domain. *Proc. Natl. Acad. Sci. U. S. A.* 112, 10359-10364.  
20  
21  
22 566 (7) Pan, G., Xu, Z., Guo, Z., Hindra, Ma, M., Yang, D., Zhou, H., Gansemans, Y., Zhu, X.,  
23 567 Huang, Y., Zhao, .LX., Jiang, Y., Cheng, J., Van Nieuwerburgh, F., Suh, J.W., Duan, Y.,  
24 568 and Shen, B. (2017). Discovery of the leinamycin family of natural products by mining  
25 569 actinobacterial genomes. *Proc. Natl. Acad. Sci. U. S. A.* 114, E11131-E11140.  
26  
27  
28 570 (8) Nett, M., Ikeda, H., and Moore, B.S. (2009). Genomic basis for natural product biosynthetic  
29 571 diversity in the actinomycetes. *Nat. Prod. Rep.* 26, 1362-1384.  
30  
31  
32 572 (9) Olano, C., Méndez, C., and Salas, J.A. (2014). Strategies for the design and discovery of  
33 573 novel antibiotics using genetic engineering and genome mining. In *Antimicrobial compounds:  
34 574 current strategies and new alternatives*, T.G. Villa and P. Veiga-Crespo, eds. (Berlin,  
35 575 Springer). pp. 1-25.  
36  
37  
38 576 (10) Rutledge, P.J. and Challis, G.L. (2015). Discovery of microbial natural products by activation  
39 577 of silent biosynthetic gene clusters. *Nat. Rev. Microbiol.* 13, 509-523.  
40  
41  
42 578 (11) Sekurova, O.N., Schneider, O., and Zotchev, S.B. (2019). Novel bioactive natural products  
43 579 from bacteria via bioprospecting, genome mining and metabolic engineering. *Microb.*  
44 580 *Biotechnol.* 12, 828-844.  
45  
46  
47 581 (12) Ye, S., Molloy, B., Braña, A.F., Zabala, D., Olano, C., Cortés, J., Morís, F., Salas, J.A., and  
48 582 Méndez, C. (2017). Identification by genome mining of a type I polyketide gene cluster from  
49 583 *Streptomyces argillaceus* involved in the biosynthesis of pyridine and piperidine alkaloids  
50 584 argimycins P. *Front. Microbiol.* 8, 194.  
51  
52  
53 585 (13) Méndez, C., González-Sabín, J., Morís, F., and Salas, J.A. (2015). Expanding the chemical  
54 586 diversity of the antitumoral compound mithramycin by combinatorial biosynthesis and  
55 587 biocatalysis: the quest for mithralogs with improved therapeutic window. *Planta Med.* 81,  
56 588 1326-1338.  
57  
58  
59  
60

- 1  
2  
3 589 (14) Becerril, A., Álvarez, S., Braña, A.F., Rico, S., Díaz, M., Santamaría, R.I., Salas, J.A., and  
4 590 Méndez, C. (2018). Uncovering production of specialized metabolites by *Streptomyces*  
5 591 *argillaceus*: activation of cryptic biosynthesis gene clusters using nutritional and genetic  
6 592 approaches. *PLoS One* 13, e0198145.
- 7  
8  
9 593 (15) Tang, G.L., Cheng, Y.Q., and Shen, B. (2004). Leinamycin biosynthesis revealing  
10 594 unprecedented architectural complexity for a hybrid polyketide synthase and nonribosomal  
11 595 peptide synthetase. *Chem. Biol.* 11, 33-45.
- 12  
13  
14 596 (16) Bode, H.B., Bethe, B., Hofs, R., and Zeeck, A. (2002). Big effects from small changes:  
15 597 possible ways to explore nature's chemical diversity. *Chembiochem* 3, 619-627.
- 16  
17  
18 598 (17) Hawkes, G.E., Herwig, K., and Roberts, J.D. (1974). Nuclear magnetic resonance  
19 599 spectroscopy. Use of carbon-13 spectra to establish configurations of oximes. *J. Org. Chem.*  
20 600 39, 1017-1028.
- 21  
22  
23 601 (18) Kajiro, H., Mitamura, S., Mori, A., and Hiyama, T. (1999). A practical synthesis of (1*S*,2*R*)-1-  
24 602 amino-2-indanol, a key component of an HIV protease inhibitor, indinavir. *Bull. Chem. Soc.*  
25 603 *Jpn.* 72, 1093-1100.
- 26  
27  
28 604 (19) Elyashberg, M.E., Blinov, K.A., and Williams, A.J. (2009). The application of empirical  
29 605 methods of <sup>13</sup>C NMR chemical shift prediction as a filter for determining possible relative  
30 606 stereochemistry. *Magn. Reson. Chem.* 47, 333-341.
- 31  
32  
33 607 (20) Huang, S.X., Yun, B.S., Ma, M., Basu, H.S., Church, D.R., Ingenhorst, G., Huang, Y., Yang,  
34 608 D., Lohman, J.R., Tang, G.L., Ju, J., Liu, T., Wilding, G., and Shen, B. (2015). Leinamycin  
35 609 E1 acting as an anticancer prodrug activated by reactive oxygen species. *Proc. Natl. Acad.*  
36 610 *Sci. U. S. A.* 112, 8278-8283.
- 37  
38  
39 611 (21) Chen, H.P., Zhao, Z.Z., Li, Z.H., Dong, Z.J., Wei, K., Bai, X., Zhang, L., Wen, C.N., Feng, T.,  
40 612 and Liu, J.K. (2016). Novel natural oximes and oxime esters with a vibr lactone backbone  
41 613 from the basidiomycete *Boreostereum vibrans*. *ChemistryOpen* 5, 142-149.
- 42  
43  
44 614 (22) Zhang, J.H., Quigley, N.B., and Gross, D.C. (1995). Analysis of the *syrB* and *syrC* genes of  
45 615 *Pseudomonas syringae* pv. *syringae* indicates that syringomycin is synthesized by a  
46 616 thiotemplate mechanism. *J. Bacteriol.* 177, 4009-4020.
- 47  
48  
49 617 (23) Rausch, C., Weber, T., Kohlbacher, O., Wohlleben, W., and Huson, D.H. (2005). Specificity  
50 618 prediction of adenylation domains in nonribosomal peptide synthetases (NRPS) using  
51 619 transductive support vector machines (TSVMs). *Nucleic Acids Res.* 33, 5799-5808.
- 52  
53  
54 620 (24) Stachelhaus, T., Mootz, H.D., and Marahiel, M.A. (1999). The specificity-conferring code of  
55 621 adenylation domains in nonribosomal peptide synthetases. *Chem. Biol.* 6, 493-505.
- 56  
57  
58  
59  
60



- 1  
2  
3 622 (25) Vaillancourt, F.H., Yin, J., and Walsh, C.T. (2005). SyrB2 in syringomycin E biosynthesis is a  
4 nonheme Fe<sup>II</sup> alpha-ketoglutarate- and O<sub>2</sub>-dependent halogenase. *Proc. Natl. Acad. Sci. U.*  
5 623 *S. A.* 102, 10111-10116.  
6 624  
7  
8 625 (26) Singh, G.M., Vaillancourt, F.H., Yin, J., and Walsh, C.T. (2007). Characterization of SyrC, an  
9 626 aminoacyltransferase shuttling threonyl and chlorothreonyl residues in the syringomycin  
10 627 biosynthetic assembly line. *Chem. Biol.* 14, 31-40.  
11  
12 628 (27) Vaillancourt, F.H., Yeh, E., Vosburg, D.A., O'Connor, S.E., and Walsh, C.T. (2005). Cryptic  
13 629 chlorination by a non-haem iron enzyme during cyclopropyl amino acid biosynthesis. *Nature*  
14 630 436, 1191-1194.  
15  
16 631 (28) Marshall, C.G., Hillson, N.J., and Walsh, C.T. (2002). Catalytic mapping of the vibriobactin  
17 632 biosynthetic enzyme VibF. *Biochemistry* 41, 244-250.  
18  
19 633 (29) Schneider, T.L., Shen, B., and Walsh, C.T. (2003). Oxidase domains in epothilone and  
20 634 bleomycin biosynthesis: thiazoline to thiazole oxidation during chain elongation.  
21 635 *Biochemistry* 42, 9722-9730.  
22  
23 636 (30) Xu, W., Qiao, K., and Tang, Y. (2013). Structural analysis of protein–protein interactions in  
24 637 type I polyketide synthases. *Crit. Rev. Biochem. Mol. Biol.* 48, 98–122.  
25  
26 638 (31) Huang, Y., Tang, G.L., Pan, G., Chang, C.Y., and Shen, B. (2016). Characterization of the  
27 639 ketosynthase and acyl carrier protein domains at the Lnml nonribosomal peptide synthetase-  
28 640 polyketide synthase interface for leinamycin biosynthesis. *Org. Lett.* 18, 4288-4291.  
29  
30 641 (32) Helfrich, E.J. and Piel, J. (2016). Biosynthesis of polyketides by trans-AT polyketide  
31 642 synthases. *Nat. Prod. Rep.* 33, 231-316.  
32  
33 643 (33) Calderone, C.T., Kowtoniuk, W.E., Kelleher, N.L., Walsh, C.T., and Dorrestein, P.C. (2006).  
34 644 Convergence of isoprene and polyketide biosynthetic machinery: isoprenyl-S-carrier proteins  
35 645 in the pksX pathway of *Bacillus subtilis*. *Proc. Natl. Acad. Sci. U. S. A.* 103, 8977-8982.  
36  
37 646 (34) Yadav, G., Gokhale, R.S., and Mohanty, D. (2003). Computational approach for prediction of  
38 647 domain organization and substrate specificity of modular polyketide synthases. *J. Mol. Biol.*  
39 648 328, 335–363.  
40  
41 649 (35) Lambalot, R.H., Gehring, A.M., Flugel, R.S., Zuber, P., LaCelle, M., Marahiel, M.A., Reid, R.,  
42 650 Khosla, C., and Walsh, C.T. (1996). A new enzyme superfamily- the phosphopantetheinyl  
43 651 transferases. *Chem. Biol.* 3, 923-936.  
44  
45 652 (36) Heathcote, M.L., Staunton, J., and Leadlay, P.F. (2001). Role of type II thioesterases:  
46 653 evidence for removal of short acyl chains produced by aberrant decarboxylation of chain  
47 654 extender units. *Chem. Biol.* 8, 207–220.  
48  
49  
50  
51  
52  
53  
54  
55  
56  
57  
58  
59  
60

- 1  
2  
3 655 (37) Garcia, I., Vior, N.M., González-Sabín, J., Braña, A.F., Rohr, J., Moris, F., Méndez, C., and  
4 656 Salas, J.A. (2013). Engineering the biosynthesis of the polyketide-nonribosomal peptide  
5 657 collismycin A for generation of analogs with neuroprotective activity. *Chem. Biol.* 20, 1022-  
6 658 1032.  
7  
8  
9  
10 659 (38) Song, L., Laureti, L., Corre, C., Leblond, P., Aigle, B., and Challis, G.L. (2014). Cytochrome  
11 660 P450-mediated hydroxylation is required for polyketide macrolactonization in stambomycin  
12 661 biosynthesis. *J Antibiot (Tokyo)*. 67, 71-76.  
13  
14 662 (39) Simunovic, V. and Müller, R. (2007). 3-hydroxy-3-methylglutaryl-CoA-like synthases direct  
15 663 the formation of methyl and ethyl side groups in the biosynthesis of the antibiotic  
16 664 myxovirescin A. *Chembiochem* 8, 497-500.  
17  
18 665 (40) Rudolf, J.D., Chang, C.Y., Ma, M., and Shen, B. (2017). Cytochromes P450 for natural  
19 666 product biosynthesis in *Streptomyces*: sequence, structure, and function. *Nat. Prod. Rep.* 34,  
20 667 1141-1172.  
21  
22 668 (41) Maier, S., Pflüger, T., Loesgen, S., Asmus, K., Brötz, E., Paululat, T., Zeeck, A., Andrade,  
23 669 S., and Bechthold, A. (2014). Insights into the bioactivity of mensacarcin and epoxide  
24 670 formation by MsnO8. *Chembiochem* 15, 749-756.  
25  
26 671 (42) Asai, A., Hara, M., Kakita, S., Kanda, Y., Yoshida, M., Saito, H., and Saitoh, Y. (1996). Thiol-  
27 672 mediated DNA alkylation by the novel antitumor antibiotic leinamycin. *J. Am. Chem. Soc.*  
28 673 118, 6802-6803.  
29  
30 674 (43) Imber, M., Pietrzyk-Brzezinska, A.J., and Antelmann, H. (2019). Redox regulation by  
31 675 reversible protein S-thiolation in Gram-positive bacteria. *Redox Biol.* 20, 130-145.  
32  
33 676 (44) Jothivasan, V.K., and Hamilton, C.J. (2008). Mycothiol: synthesis, biosynthesis and  
34 677 biological functions of the major low molecular weight thiol in actinomycetes. *Nat. Prod. Rep.*  
35 678 25, 1091-1117.  
36  
37 679 (45) Schallmey, M., Floor, R.J., Szymanski, W., and Janssen, D.B. (2012). Hydrolysis and  
38 680 reverse hydrolysis: halohydrin dehalogenases. In *Comprehensive chirality*, Carreira, E.M.  
39 681 and Yamamoto, H. eds. (Amsterdam, Elsevier), pp. 143–155.  
40  
41  
42  
43  
44  
45  
46  
47  
48  
49  
50  
51  
52  
53  
54  
55  
56  
57  
58  
59  
60



254x190mm (96 x 96 DPI)